J Neurophysiol 109: 3013–3024, 2013.
First published March 20, 2013; doi:10.1152/jn.01021.2012.

Binocular integration and disparity selectivity in mouse primary visual cortex

Benjamin Scholl, Johannes Burge, and Nicholas J. Priebe
Center for Perceptual Systems, Section of Neurobiology, School of Biological Sciences, College of Natural Sciences, The University of Texas at Austin, Austin, Texas

Submitted 26 November 2012; accepted in final form 18 March 2013

Scholl B, Burge J, Priebe NJ. Binocular integration and disparity selectivity in mouse primary visual cortex. *J Neurophysiol* 109: 3013–3024, 2013. First published March 20, 2013; doi:10.1152/jn.01021.2012.—Signals from the two eyes are first integrated in primary visual cortex (V1). In many mammals, this binocular integration is an important first step in the development of stereopsis, the perception of depth from disparity. Neurons in the binocular zone of mouse V1 receive inputs from both eyes, but it is unclear how that binocular information is integrated and whether this integration has a function similar to that found in other mammals. Using extracellular recordings, we demonstrate that mouse V1 neurons are tuned for binocular disparities, or spatial differences, between the inputs from each eye, thus extracting signals potentially useful for estimating depth. The disparities encoded by mouse V1 are significantly larger than those encoded by cat and primate. Interestingly, these larger disparities correspond to distances that are likely to be ecologically relevant in natural viewing, given the stereo-geometry of the mouse visual system. Across mammalian species, it appears that binocular integration is a common cortical computation used to extract information relevant for estimating depth. As such, it is a prime example of how the integration of multiple sensory signals is used to generate accurate estimates of properties in our environment.

primary visual cortex; mouse binocularity; disparity tuning; ocular dominance

TO ENABLE ACCURATE ESTIMATES of behaviorally relevant properties of the environment, sensory systems integrate information from multiple sources. For example, in the visual system, signals from the left and right eyes are integrated to provide information about depth. In mammals, left and right eye signals first converge in primary visual cortex (V1). The different vantage points of the eyes create local spatial offsets in the retinal images, offsets known as binocular disparities. Binocular disparity changes with the depths of objects in the environment. Neurons that encode retinal image information relevant for estimating binocular disparity therefore provide information relevant for binocular depth perception (Barlow et al. 1967; Blakemore 1969; Hubel and Wiesel 1973; Joshua 1970; Nikara et al. 1968; Pettigrew et al. 1968). Binocular disparity selectivity can be observed in individual neurons; some binocular stimuli elicit large increases in responses, while others reduce responses, relative to monocular stimulation alone (Hubel and Wiesel 1962; Ohzawa and Freeman 1986; Pettigrew et al. 1968).

Disparity-selective binocular neurons have been reported in many animals, including carnivores and primates. Such neurons have not, however, been reported in rodents. In recent years, mice have become an increasingly important model for the study of visual processing and cortical plasticity. Genetic techniques are now available to dissect underlying circuitry and its emergence during development. Here, we report evidence that mice have binocular neurons strikingly similar to those underlying depth perception in other mammals.

Mouse V1 is comprised of two zones: the monocular zone, where individual neurons respond only to the contralateral eye, and the binocular zone, where neurons respond to stimulation of either eye (Dräger 1975; Kalatsky and Stryker 2003; Schuett et al. 2002; Wagor et al. 1980). To date, binocularity in rodent V1 has been characterized by measuring ocular dominance: the difference in spiking response strength elicited by stimulating each eye separately (Gordon and Stryker 1996; Hanover et al. 1999; Hofer et al. 2006; Hubel and Wiesel 1962; Mrsic-Flogel et al. 2007; Tagawa et al. 2005). Because ocular dominance is measured by independent stimulation of each eye, it does not reveal the nature of binocular integration. It is therefore unknown whether mouse V1 neurons integrate binocular information that could provide a basis for stereoscopic depth perception (Huberman and Niell 2011).

Mouse binocularity may be unrelated to binocular disparity selectivity and may reflect the use of independent signals from each eye to improve signal detection (Anderson and Movshon 1989; Legge 1984; Pardhan and Rose 1999; Simpson et al. 2009). Our records, however, are inconsistent with the hypothesis that binocularity exists solely to improve signal detection. Rather, our records indicate that binocular neurons in mouse V1 are selective for binocular disparity. A detailed comparison of mouse and cat disparity selectivity reveals that mouse neurons are modulated less by binocular disparity. A simple threshold-linear model based on monocular responses alone accounts for much of the binocular responses in both mouse and cat V1 simple cells. These recordings demonstrate that a common pattern of binocular integration occurs in V1 across mammalian species.

METHODS

Physiology. Physiological procedures for mouse recordings were based on those previously described (Tan et al. 2011). All our experiments were conducted with adult C57BL/6 mice (age 5–8 wk). Mice were anesthetized with intraperitoneal injection of either 50–80 mg/kg pentobarbital sodium ($n = 7$) or 1,000 mg/kg urethane ($n = 7$) and with intramuscular injection of 10 mg/kg chlorprothixene; the dose of pentobarbital sodium or urethane was adjusted during the procedure to eliminate the pedal withdrawal reflex. Brain edema was prevented by intraperitoneal injection of 20 mg/kg dexamethasone. Animals were warmed with a thermostatically controlled heat lamp to maintain body temperature at 37°C. A tracheotomy was performed. The head was placed in a mouse adaptor (Stoelting), and a craniotomy and duratomy were preformed over visual cortex. Mouse eyes were kept moist with either frequent application of artificial tears or a thin layer of silicone oil. V1 was located and mapped by multiunit extracellular recordings with Parylene-coated tungsten electrodes

Address for reprint requests and other correspondence: N. J. Priebe, Section of Neurobiology, Univ. of Texas at Austin, 2400 Speedway, Austin, TX 78712 (e-mail: nicholas@mail.utexas.edu).

(Micro Probe). The boundaries of V1 and V2 were identified by the characteristic gradient in receptive locations (Dräger 1975; Métin et al. 1988). The binocular zone of V1 was located by identifying receptive fields in the center of the binocular visual field and verifying by stimulating contralateral and ipsilateral eyes independently (Gordon and Stryker 1996). Eye drift under urethane anesthesia is typically small and results in a change in eye position of $<2°$/h (Sarnaik et al. 2013).

The physiological procedures for cat experiments were based on those previously described (Tan et al. 2011). Briefly, anesthesia was induced with ketamine (5–15 mg/kg) and acepromazine (0.7 mg/kg) followed by intravenous administration of a mixture of propofol and sufentanil. Once a tracheotomy was performed the animal was placed in a stereotaxic frame for the duration of the experiment. Recording stability was increased by suspending the thoracic vertebrae from the stereotactic frame and performing a pneumothoracotomy. Eye drift was minimized with intravenous infusion of vecuronium bromide. Anesthesia was maintained during the course of the experiment with continuous infusion of propofol and sufentanil (6–9 $mg \cdot kg^{-1} \cdot h^{-1}$ and 1–1.5 $\mu g \cdot kg^{-1} \cdot h^{-1}$, respectively). Body temperature, electrocardiogram, EEG, CO_2, blood pressure, and autonomic signs were continuously monitored and maintained. The nictitating membrane was retracted with phenylephrine hydrochloride, and the pupils were dilated with topical atropine. Contact lenses were inserted to protect the corneas. Supplementary lenses were selected by direct ophthalmoscopy to focus the display screen onto the retina.

Extracellular recordings. Extracellular electrodes (1–2 MΩ, Micro Probes) were advanced into cortex (cat: area 17, ~2 mm lateral of midline; mouse: binocular zone) with a motorized drive (MP-285, Sutter Instrument). After the electrode was in place, warm agarose solution (2–4% in normal saline) was placed over the craniotomy to protect the surface of the cortex and reduce pulsations. Action potentials were identified with a dual window discriminator (Bak Electronics, DDIS-1). The time of action potentials and raw extracellular traces were recorded for later analysis.

Stimuli. Visual stimuli were generated by a Macintosh computer (Apple) using the Psychophysics Toolbox (Brainard 1997; Pelli 1997) for MATLAB (MathWorks) and presented dichoptically with two Sony video monitors (GDM-F520) placed either 50 cm (cat) or 38 cm (mouse) from the animal's eyes. The video monitors had a noninterlaced refresh rate of 100 Hz and a spatial resolution of 1,024 × 768 pixels, which subtended 40 × 30 cm (56° × 43° in mouse, 44° × 34° in cat). The video monitors had a mean luminance of 40 cd/cm^2. Drifting grating stimuli were presented for either 1.5 s (mouse) or 4 s (cat), preceded and followed by 250-ms blank (mean luminance) periods. Spontaneous activity was measured with blank periods interleaved with drifting grating stimuli and lasting the same duration (1.5–2 s or 4 s). Stimulus duration was typical for measurements in V1 of mouse (Gao et al. 2010; Niell and Stryker 2008) and cat (Priebe 2008), as neurons in mouse V1 show stronger response adaptation. In mouse recordings we characterized stimulus orientation in the contralateral eye and used full-field gratings of low spatial frequency [0.03–0.06 cycles per degree (cpd)] to stimulate cell receptive fields (5–30° diameter), which are generally larger than those in cat (Bonin et al. 2011; Dräger 1975; Gordon and Stryker 1996; Mangini and Pearlman 1980; Métin et al. 1988). Orientation and spatial frequency measured in the contralateral eye were used in the ipsilateral eye, because stimulus selectivity for each eye matches (Wang et al. 2010). Ipsilateral receptive field locations in mouse were mapped with multiunit activity because the spiking responses of single neurons are often small or nonexistent to ipsilateral stimulation. Receptive field size was mapped for the contralateral eye, and stimulus size was 1–3° larger than the classic receptive field of each neuron. For the ipsilateral eye we used a large stimulus to guarantee stimulation (24–29°). Mean stimulus sizes for contralateral and ipsilateral eyes were 23.5 ± 8.1° and 24.9 ± 8.7°, respectively. In 27% of our recordings, stimulus size differed by >2°, with a mean difference of 4.6°. In mouse V1, surround suppression of visual responses were generally avoided because surround suppression measured previously required a stimulus size >33° in diameter (Gao et al. 2010) and here stimuli did not extend 29° in diameter. For cat recordings we initially characterized stimulus orientation, spatial frequency (0.20–0.85 cpd), spatial location, and size (0.5–2° diameter) best evoking a response in the eye that elicited the strongest response. Binocular stimuli were presented dichoptically (Fig. 1*A*) with the preferred stimulus parameters at 2–4 Hz temporal frequency and 90% contrast. A mirror was placed directly in front of the contralateral eye to reflect receptive field locations onto a separate monitor. The angle and location of the mirror were adjusted to avoid occlusion of the field of view for the ipsilateral eye. With the mirror in place, receptive field locations for each eye were mapped again and dichoptic stimulation was verified. To measure binocular interactions we systematically changed the spatial phase of one grating while holding the spatial phase of the other grating constant. Relative phase disparities used ranged from −180° to 135°. With a 0.05-cpd sine-wave grating, a 90° phase disparity corresponds to a disparity of 5° of visual angle. All binocular and

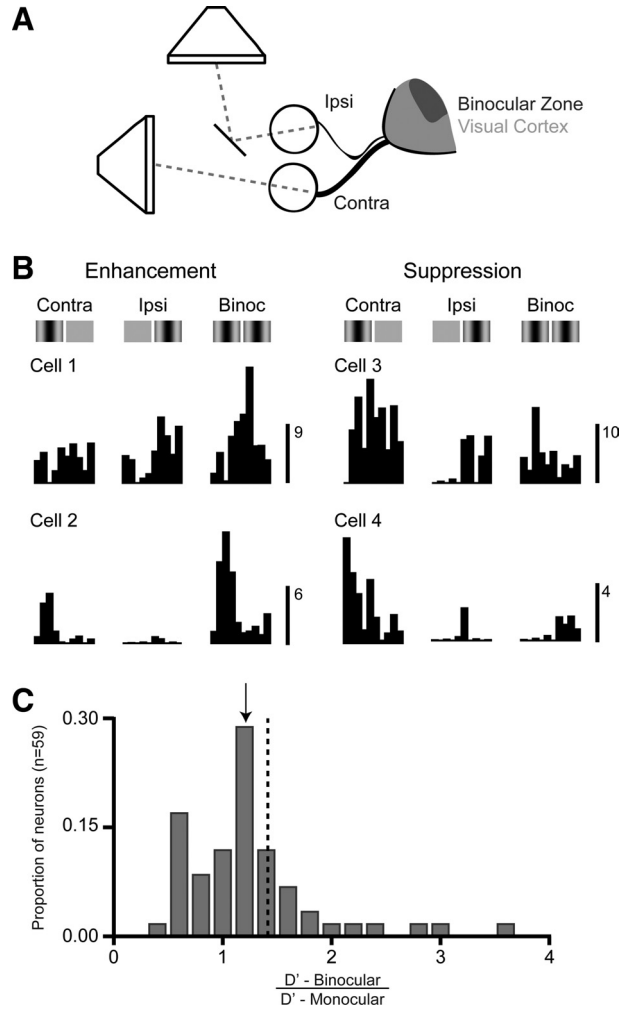

Fig. 1. Dichoptic stimulation in mouse primary visual cortex (V1) neurons shows enhancement and suppression. *A*: schematic of methods for dichoptic stimulation and organization of binocular zone in mouse V1. *B*: mouse V1 neurons responding to contralateral and ipsilateral stimulation show enhanced (*left*) or suppressed (*right*) binocular responses. Scale bars indicate spike rate (spikes per second). *C*: distribution of ratios of response detection sensitivity of mouse V1 neurons under binocular and monocular stimulation. Arrow indicates geometric mean, and dashed line shows expectation for dichoptic detection sensitivity.

monocular stimuli were presented during the same block and pseudorandomly interleaved.

Analysis. Spiking responses for each stimulus were cycle averaged across trials after removal of the first cycle. The Fourier transform was used to calculate the mean (F_0) and modulation amplitude (F_1) of each cycle-averaged response, and after, mean spontaneous activity was subtracted. Simple and complex cells were separated by computing the modulation ratio (F_1/F_0) to the preferred monocular stimulus; those neurons with modulation ratios >1 are considered simple. Peak responses were defined as the sum of the mean and modulation ($F_0 + F_1$). The threshold-linear model (*Eq. 6*) was fit to the peak responses of individual neurons by adjusting the gain of the contralateral and ipsilateral inputs, the phase of those inputs, and the threshold. The mean-squared error between the model fit and the recorded spiking data was minimized with the MATLAB function lsqcurvefit.

All procedures were approved by The University of Texas at Austin Institutional Animal Care and Use Committee.

RESULTS

Neuronal responses to binocular stimulation in mouse V1. To explore binocular integration in mouse V1 and compare it to that found in cat V1, we made extracellular single-unit recordings in anesthetized animals. In mice, we first mapped V1 to find the binocular zone. We selected receptive field locations within the central 30° of the visual field, where there is clear overlap of left and right eye projections. In cats, recordings were made from the central 15° of vision, where most neurons receive binocular inputs. Here we report records from 68 mouse V1 neurons and 69 cat V1 neurons. Drifting sine-wave gratings were presented in both monocular and binocular conditions. Gratings were presented binocularly by placing a mirror in front of one eye so that each eye could be stimulated by a visual stimulus presented on a separate monitor (Fig. 1*A*).

Mouse V1 neurons in the binocular zone are known to receive inputs from both eyes, but it is unknown how these neurons respond to binocular stimulation. We first compared how neurons responded to drifting gratings during monocular and binocular stimulation, using the same drifting gratings since neuronal stimulus preferences for each eye are matching (Wang et al. 2010) (see METHODS). For some cortical neurons, binocular stimulation led to a dramatic response enhancement relative to the responses elicited by monocular stimulation (Fig. 1*B*, *left*). For other neurons, binocular stimulation resulted in a profound response suppression relative to the responses evoked monocularly (Fig. 1*B*, *right*). Interestingly, similar patterns of responses were observed even for neurons that would be considered monocular from their responses to each eye alone (Fig. 1*B*, *bottom*).

If binocularity in mouse V1 acted solely to increase signal detection sensitivity, binocular stimuli should be more detectable than monocular stimuli by a factor of $\sqrt{2}$ (Anderson and Movshon 1989; Legge 1984; Pardhan and Rose 1999; Simpson et al. 2009). Because the error of n measurements decreases in proportion to $\sqrt{n}$, we expect sensitivity to increase by $\sqrt{2}$ using two eyes. We tested whether there was increased sensitivity for binocular stimulation compared with monocular (contralateral) stimulation across all mouse records by computing the changes in signal detection sensitivity (d') for monocular (contralateral) and binocular stimulation:

$$d' = \frac{\mu_{resp} - \mu_{spont}}{\frac{1}{2}\sqrt{\sigma^2_{resp} + \sigma^2_{spont}}} \quad (1)$$

where μ_{resp} and σ_{resp} are the response mean and variance during visual stimulation and μ_{spont} and σ_{spont} are the spontaneous activity mean and variance during mean luminance periods (Simpson and Fitter 1973; Swets 1986). Binocular and monocular response detection sensitivity were similar on average across mouse V1 neurons ($d'_{binocular}$ = 1.12 ± 0.55 SD, d'_{contra} = 1.02 ± 0.61 SD; $P < 0.25$). The ratio of d' for monocular and binocular stimulus conditions for V1 neurons (geometric mean = 1.10 ± 0.22 SD) was less than expected ($\sqrt{2}$) under a signal detection improvement hypothesis and was highly variable across neurons (Fig. 1*C*). These results suggest that binocularity in mouse V1 neurons does not function solely to increase signal detection.

The observed diversity in d' values may be due to binocular receptive fields that compare between inputs from each eye and are selective for binocular disparity. For some neurons the particular binocular stimulus employed is matched to their binocular disparity preference and thus evoked response enhancement (62%). For other neurons, the binocular stimulus is mismatched to their binocular disparity preference and suppressed responses (34%). As in carnivores and primates, the spatial configuration of stimuli in each eye—particularly the binocular disparity of the stimulus between the eyes—along with the specific receptive field configuration of each neuron may determine whether responses are enhanced or suppressed during binocular stimulation (Ohzawa and Freeman 1986).

Our analysis of d' is meant to mimic a natural detection task, in which the stimulus would activate some neurons more than others depending on the depth of the object. If we find a binocular stimulus that best evokes a response for each neuron, the ratio of d' for monocular and chosen binocular conditions increases substantially (geometric mean = 1.8 ± 0.78 SD). On the other hand, if we select the binocular condition evoking the weakest response in each neuron, the d' ratio declines (geometric mean = 0.82 ± 0.54 SD). Changes in d' ratios measured by tailoring the spatial configuration of binocular stimuli for each neuron suggest that the neurons are selective for binocular disparity and indicate that it is important to measure how mouse binocular neurons respond to a range of binocular disparities.

Binocular cues for depth in mice. The response properties of binocular neurons in mouse V1 should be strongly influenced by signals that stimulate the visual system, and the tasks for which those signals are used in natural viewing. Here, we consider how the response properties of binocular neurons might be shaped by natural signals, under the assumption that binocular neurons in mouse V1 support binocular depth perception (i.e., stereopsis). Canonical V1 binocular neurons are selective for disparity but are not invariant; that is, their responses are strongly modulated both by disparity and by spatial frequency content. Thus the V1 population should encode the retinal image information relevant for estimating disparity. Subsequent decoding (i.e., disparity estimation) may result in neural populations that are both selective and invariant (Burge J, Geisler WS, unpublished observations).

Here, we show how the stereo-geometry of the mouse visual system (Fig. 2*A*) can be used to predict the spatial frequency selectivity of mouse binocular neurons. The predictions are in line with previous neurophysiological measurements of these neurons (Fig. 2*C*) (Niell and Stryker 2008; Vreysen et al. 2012). The stereo-geometry of the mouse visual system determines the range of binocular disparities that may stimulate the mouse visual system and, therefore, that may be useful to encode.

Binocular disparities, the local differences between the retinal images, arise because of the different viewing positions of each eye. The binocular disparity (δ), in visual angle, of corresponding points in the left and right eyes is defined as

$$\delta = \alpha_L - \alpha_R \quad (2)$$

where α_L and α_R are the angles between the retinal projections of a target and the preferred binocular locus (defined below) in the left and right eyes. The functional relationship between binocular disparity (in radians) and depth, under the small angle approximation, is given by

$$\delta = \frac{-\Delta I}{(d_{pref} + \Delta)d_{pref}} = \frac{-I}{\left(\frac{d_{pref}}{\Delta} + 1\right)d_{pref}} \quad (3)$$

where I is the interocular distance, d_{pref} is the preferred binocular viewing distance, and Δ is the depth of an object. Depth is defined as the difference between the object and the preferred viewing distance (d_{pref}): $\Delta = d_{object} - d_{pref}$, where d_{pref} is the viewing distance at which a target will project onto the retinas at the preferred binocular locus, the corresponding retinal locations where disparity estimates are most precise. In primates and carnivores that binocular locus is the fovea or area centralis, and the preferred binocular viewing distance is the current fixation distance. Mice do not have a well-defined fovea, so it is not straightforward to determine the viewing distance at which disparity would be encoded with the greatest precision.

It is possible, however, to place constraints on the preferred binocular viewing distance by considering three facts about mouse vision. First, mice typically have +10.0 diopters of refractive error (de la Cera et al. 2006), which means that targets positioned at 10 cm will be in best focus. Second, mice are largely unable to change the refractive power of their eyes (Chalupa and Williams 2008). Third, mice have limited eye movements (Chalupa and Williams 2008). Together these facts about the mouse visual system suggest that the preferred binocular viewing distance is fixed straight ahead at a distance of 10 cm (Fig. 2, *A* and *B*). For the analysis that follows, we assume that this distance is the preferred operating range for mouse binocular vision. Note that because of the difficulty refracting small eyes, there may be an effective refractive error somewhat different from 10 diopters. Modest changes in this value do not qualitatively affect our conclusions.

To determine the widest range of disparities that could potentially stimulate the mouse visual system, we first consider the largest uncrossed disparity that could be formed in the mouse visual system. The largest uncrossed disparity is created by an object at infinity. With a mouse interocular separation of 1 cm and a preferred binocular viewing distance of 10 cm, the largest possible uncrossed disparity is −5.7° (*Eq. 3*). Uncrossed disparities with magnitudes larger than −5.7° are "impossible" disparities because they could never be generated in natural viewing. Assuming symmetrical disparity encoding (±5.7°), disparity would provide mice useful binocular depth information over a range of distances from 5 cm to infinity. This range of disparities is significantly larger than the dispar-

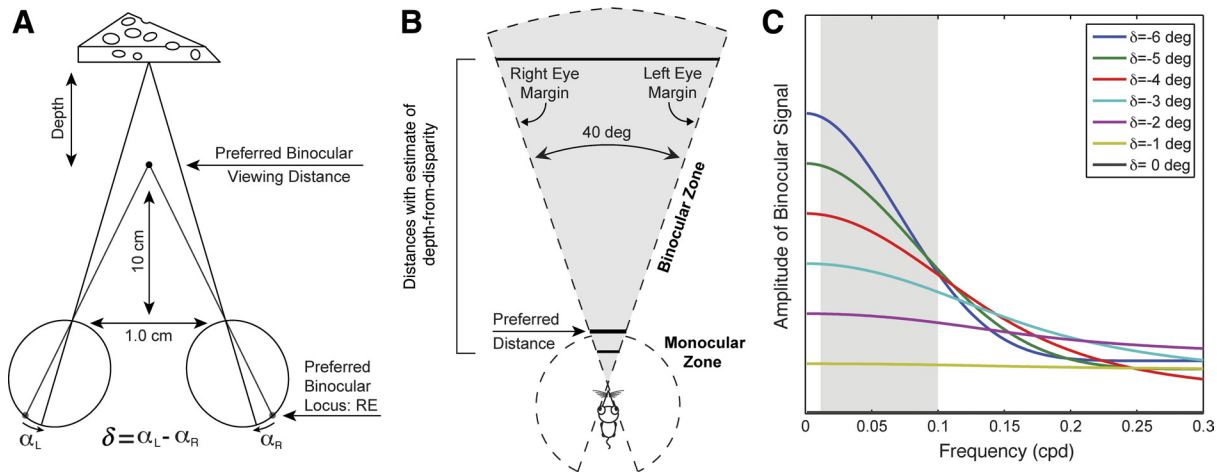

Fig. 2. Stereo-geometry, spatial frequencies with disparity information in mouse. *A*: stereo-geometry of the mouse visual system. A point on an object of interest projects to the left and right eyes. If the object is not at the preferred binocular viewing distance, binocular disparity results. The disparity of the images entering the 2 eyes is given by $\delta = \alpha_L - \alpha_R$, where α_L and α_R are the angles between the retinal projections of a point on an object and the preferred binocular locus in the left and right eyes. The preferred binocular locus is the pair of retinal locations where disparity estimates are most precise. *B*: mouse monocular and binocular visual fields. Mouse binocular visual fields subtend ~40° (Heesy 2004). Each monocular visual field subtends ~180°. Given mouse stereo-geometry, disparity would provide information about distances ranging from 5.3 to 96.3 cm, assuming mice encode 90% of the full range of possible disparities (large brackets, *Eq. 3*). This range of distances is likely to be ecologically relevant. Note that if mice encoded the same range of disparities as cat (−2.5° to +2.5°; Packwood and Gordon 1975) or primate (−1.5° to +1.5°; Blakemore 1970), the corresponding range of distances would be significantly smaller: 7.0–17.8 cm and 7.9–13.6 cm. *C*: the spatial frequencies that are useful for estimating disparities in the predicted range. Amplitude spectra of binocular difference signals (*Eq. 4*) after being filtered by 1.5-octave-bandwidth filters. Shaded region indicates the spatial frequencies [0.01–0.10 cycles per degree (cpd)] that provide the best information for estimating the disparities that are predicted to be ecologically relevant for mouse stereopsis. Higher spatial frequencies provide little information about disparity.

ity ranges encoded by the primate and cat visual systems (Fig. 2*B*), but it is the range that provides binocular depth information over a useful range of distances for mice.

The range of disparities that the mouse visual system is stimulated with in natural viewing can be used predict the range of spatial frequencies that disparity-sensitive neurons are selective for. To determine the spatial frequencies that carry useful information about disparities between ±5.7°, we examined the disparity signals that would result from a binocularly viewed high-contrast luminance edge positioned at or behind the preferred binocular viewing distance. We use a binocularly viewed edge because each eye's image of the edge has a spatial frequency spectrum that approximates the 1/f contrast fall-off that is characteristic of natural images (Field 1987). The difference between the left- and right-eye images of the edge is the binocular difference signal. At each spatial frequency, the binocular difference signal is sinusoidal with contrast amplitude given by

$$A_B(f|\delta_k) = \sqrt{A_L(f)^2 + A_R(f)^2 - 2A_L(f)A_R(f)\cos(2\pi f\delta_k)} \quad (4)$$

where f is the spatial frequency, δ_k is a particular disparity, A_L and A_R are the left and right eye retinal amplitudes, and $A_B(f|\delta_k)$ is the amplitude of the binocular difference signal (Burge J, Geisler WS, unpublished observations). Figure 2*C* shows the amplitude of this difference signal for seven disparities (−6° to 0°) spanning the range of uncrossed disparities to which mice are predicted to be sensitive. The shape and magnitude of the spectra differ systematically as a function of disparity between 0.01 and 0.1 cpd. At higher spatial frequencies, the binocular difference signals are barely distinguishable. Thus the pattern of binocular contrasts in this spatial frequency range (0.01 to 0.1 cpd) contains the information that is most useful for estimating disparities between −5.7° and 5.7°.

This analysis suggests that individual neurons are insufficient to accurately estimate binocular disparity from natural stereo-images. Individual V1 binocular neurons are sensitive only to a narrow band of frequencies (e.g., 1.5 octaves), whereas disparity information is contained in the pattern of binocular contrast across a relatively broad band of spatial frequencies. Thus, in natural images, disparity must be estimated from the pattern of population activity of many V1 neurons with different spatial frequency preferences.

Our analysis of the stereo-geometry of the mouse suggests a range of relevant spatial frequencies (0.01 to 0.1 cpd) that carries useful disparity information, which is very similar to the range of spatial frequency that mouse visual cortex encodes (Niell and Stryker 2008; Vreysen et al. 2012). It is possible that additional factors such as the optics of the eyes and the photoreceptor density provide additional constraints on the spatial frequency selectivity of V1 neurons (Banks and Bennett 1988; Burge J, Geisler WS, unpublished observations). Our analysis did not consider those factors, and it is therefore remarkable, and potentially coincidental, that the spatial frequency range we predict is matched to those encoded by V1 neurons. We nonetheless use this range of relevant spatial frequencies to guide our neurophysiological recordings, presenting drifting sine-wave gratings of low spatial frequency (0.03–0.06 cpd) to characterize disparity selectivity of individual neurons in mouse V1.

Binocular integration in mouse. We observed a variety of response patterns from V1 neurons in mouse and cat under binocular stimulation. The spiking activity of individual neurons was measured in response to eight binocular disparities (Fig. 3*A*, *left*), to monocular stimulation of the left and right eyes, and to no stimulation (Fig. 3*A*, *right*). Spiking activity to each stimulus was cycle averaged and the peak response amplitude (F_1 + DC, see METHODS) was measured for each condition (Fig. 3*A*, *bottom right*). We initially classified cells as simple and complex on the basis of the relative response modulation to monocularly presented drifting gratings (see METHODS). Among simple cells we observed a variety of responses patterns that indicate little relationship between ocular dominance and disparity tuning. The first subset of simple cells was characterized as binocular on the basis of their ocular dominance (Fig. 3, *A* and *B*). Responses from these binocular simple cells were modulated by disparity during binocular stimulation. The second subset of simple cells was characterized as monocular by ocular dominance. Surprisingly, responses from these simple cells were also modulated by binocular disparity (Fig. 3, *C* and *D*). A third subset of simple cells was characterized as binocular by ocular dominance but did not show a response modulation to the binocular stimulus (Fig. 3, *E* and *F*). These three subsets of simple cells show that binocularity based on ocular dominance and binocular disparity are not necessarily linked (Chino et al. 1994; LeVay and Voigt 1988).

The complex cells of mouse and cat showed the same variety of response patterns as simple cells. Neurons that were classified as either binocular or monocular by ocular dominance could exhibit disparity tuning (Fig. 4, *A–D*). In addition, we found complex cells that appeared binocular by ocular dominance but exhibited little response modulation to changes in binocular disparity (Fig. 4, *E* and *F*). The lack of relationship between binocularity defined by ocular dominance and by disparity sensitivity shown in these example neurons suggests that these two measures of binocularity reflect distinct neural computations.

To quantify the relationship between binocularity defined by ocular dominance and binocularity defined by disparity selectivity, we quantified the degree of binocularity for both monocular and binocular stimulus conditions across our population of neurons. For ocular dominance we used the spiking ocular dominance index (ODI_R), which compares the degree to which neurons respond to the contralateral and ipsilateral eye based on the monocular stimuli:

$$ODI_R = \frac{(R_{contra} - R_{ipsi})}{(R_{contra} + R_{ipsi})} \quad (5)$$

where R_{contra} is the peak spiking response to contralateral eyes stimulation and R_{ipsi} is the peak response to ipsilateral eye stimulation. ODI_R values of 0 indicate equal responses to each eye (Fig. 3, *A* and *B*, Fig. 4, *A* and *B*), while values of −1 and 1 indicate the dominance of the ipsilateral and contralateral eyes (Fig. 3, *C* and *D*, Fig. 4, *C* and *D*). As previously shown, mouse V1 neurons exhibit a pronounced ocular dominance bias for the contralateral eye [mean ODI_R = 0.35 ± 0.54 (SD)] (Gordon and Stryker 1996) (Fig. 5*A*).

To quantify the degree of response modulation induced by binocular stimulation we computed a disparity selectivity index

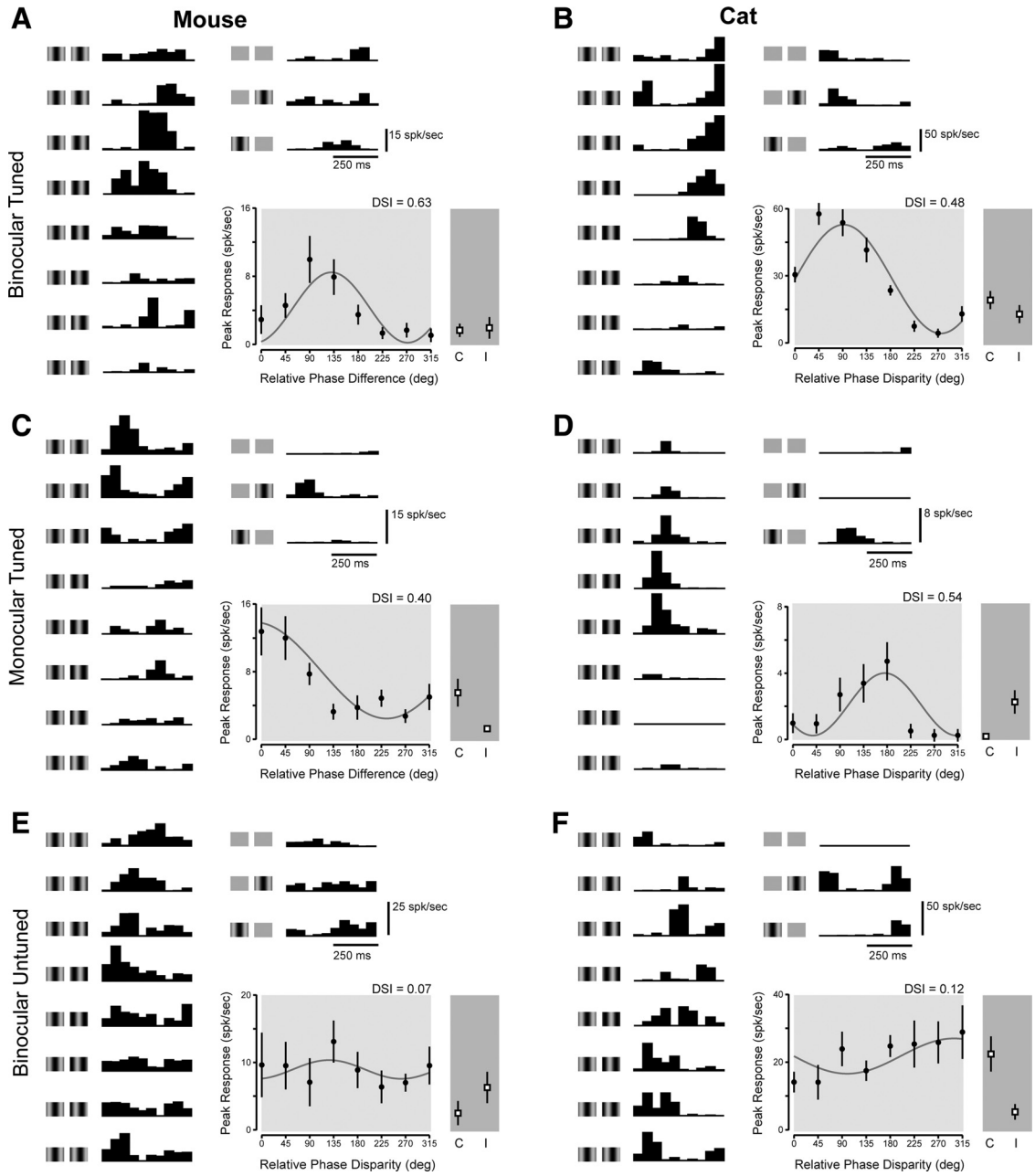

Fig. 3. Simple cell disparity selectivity in mouse and cat. *A*: binocular neurons in mouse V1 show a modulation of peak response to different spatial phase combinations of binocular stimuli. Binocular cycle-averaged responses are shown at *left*. Illustration of each stimulus condition is shown next to each response. Spontaneous activity and monocular responses are shown at *right*. Binocular tuning is plotted from peak response amplitudes of binocular responses (black dots) alongside monocular responses (squares). C indicates contralateral stimulation alone, and I indicates ipsilateral stimulation alone. *B*: same as in *A* for a neuron in cat V1. *C*: same as in *A* for a monocular neuron. *D*: same as in *C* for a neuron in cat V1. *E*: neurons in mouse V1 show no modulation in response amplitude despite responding to stimulation of either eye. *F*: same as *E* for a neuron in cat V1. DSI, disparity selectivity index.

(DSI), which describes the degree of response modulation evoked by changes in spatial phase for binocular stimuli. The DSI is based on similar measurements of orientation selectivity (Ringach et al. 2002; Tan et al. 2011):

$$\mathrm{DSI} = \frac{\sqrt{\left(\sum_\phi R_\phi \sin(\phi)\right)^2 + \left(\sum_\phi R_\phi \cos(\phi)\right)^2}}{\sum_\phi R_\phi} \qquad (6)$$

where R_ϕ indicates the peak responses to each spatial phase (ϕ). DSI values range between 0 and 1, where 0 indicates a lack of modulation by binocular disparity (Fig. 3, *E* and *F*, Fig. 4, *E* and *F*) and higher values indicate greater degrees of modulation by disparity (Fig. 3, *A–D*, Fig. 4, *A–D*).

Mouse V1 neurons are modulated by binocular stimulation, exhibiting a range of DSI values similar to that found in the cat (mouse DSI range = 0–0.7, cat range = 0–0.75). On average, however, mouse neurons were modulated less by disparity than cat neurons (mouse: mean DSI = 0.18 ± 0.18 SD, cat: mean DSI = 0.30 ± 0.18 SD; significant difference between mouse and cat, $P < 0.001$, *t*-test). Across mouse V1 neurons there was no significant difference in DSI values between simple and complex cells (Fig. 5; Student's *t*-test, $P < 0.4$), but across cat

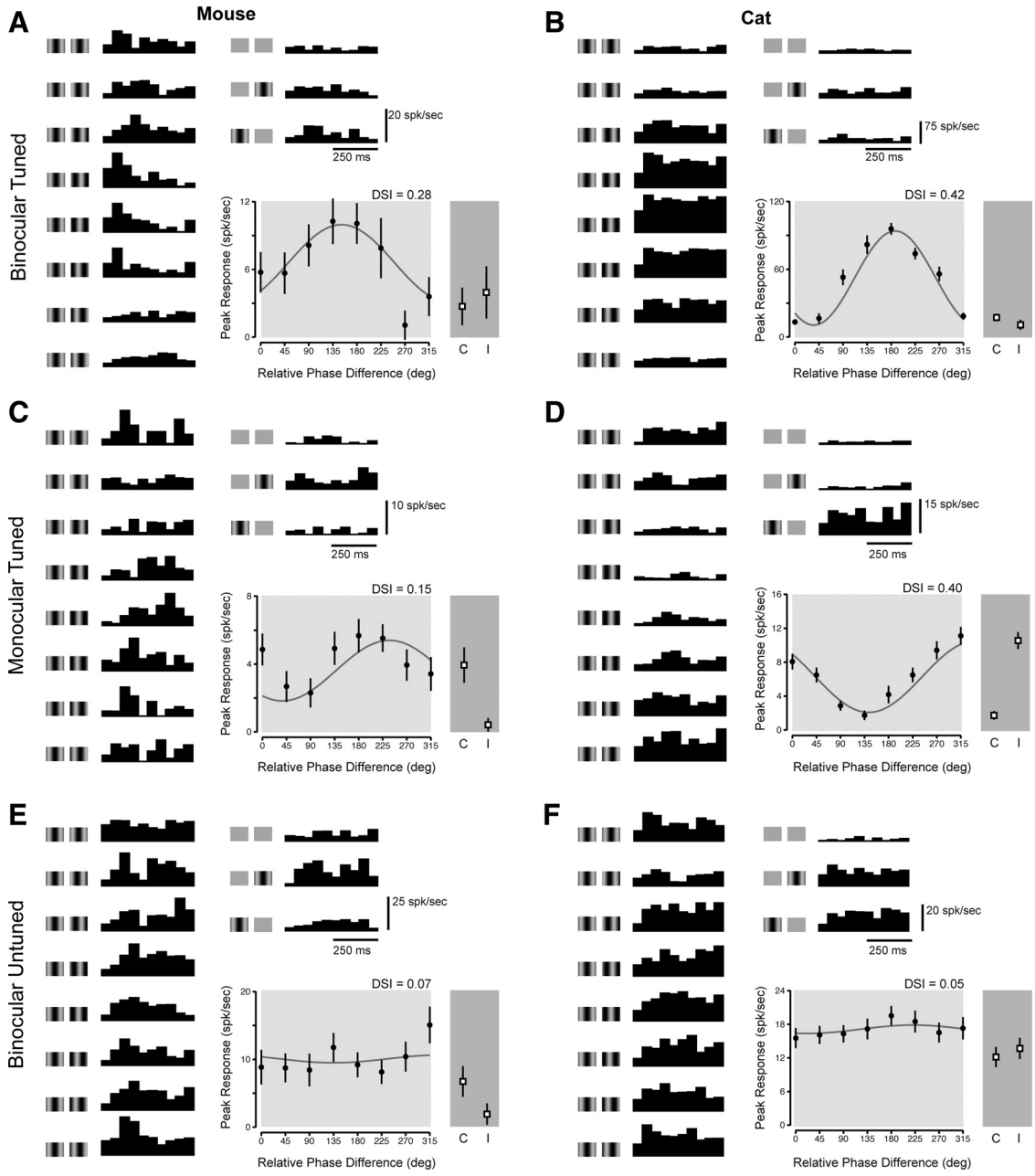

Fig. 4. Complex cell disparity selectivity in mouse and cat. *A–F*: same layout as in Fig. 3 for complex cells.

neurons there was a difference between these classes of cells (simple cell mean = 0.37 ± 0.18, complex cell mean = 0.2 ± 0.14; Student's *t*-test, $P < 0.005$), which has been reported previously (Chino et al. 1994). Computing disparity selectivity with only the modulation response component in simple cells and the mean response component in complex cells did not change the difference in DSI between cell classes (simple cell mean = 0.36 ± 0.24, complex cell mean = 0.22 ± 0.17; Student's *t*-test, $P < 0.005$).

To compare the degree of binocularity based on ocular dominance to the degree of disparity selectivity, we compared the ODI_R to the DSI metrics. We first transformed the ODI_R by taking the absolute value so that a value of 0 indicates a binocular neuron and a value of 1 a monocular neuron. No systematic relationship is evident between the two metrics in the mouse (Fig. 5*A*; slope = 0.01 ± 0.07, principal component analysis with bootstrapped standard error) or in the cat (Fig. 5*B*; slope = 0.08 ± 0.09, principal component analysis with bootstrapped standard error) (Chino et al. 1994; LeVay and Voigt 1988). The failure to observe a relationship between the absolute value of ODI_R and DSI might be due to the nonlinear relationship between the inputs a neuron receives and its spiking ouput. For example, a neuron could receive strong synaptic inputs from both eyes, but because of spike threshold only monocular stimulation to the dominant eye elicits a spiking response. In this case, the spiking ODI_R value would be near 1, indicating monocularity, despite receiving input from both eyes (Priebe 2008). Although our extracellular recordings revealed no relationship between the degree of disparity selectivity and ocular dominance, there may nonetheless exist a

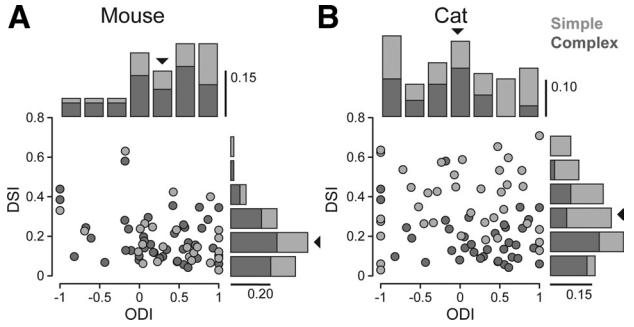

Fig. 5. Relationship between ocular dominance and disparity selectivity. Spiking ocular dominance index (ODI_R) and DSI plotted for each simple (light gray) and complex (dark gray) cell in mouse V1 (*A*) and cat V1 (*B*). Distributions for each index are shown along the same axis. Scale bars indicate proportion of cells in histograms.

relationship between these two metrics at the subthreshold level.

Modeling the binocular disparity tuning of visual cortical neurons. Our observation that mouse V1 neurons are sensitive to binocular disparity suggests that similar computations are being performed in V1 across mammals. This raises the question about how comparisons between left and right eye inputs occur. The dominant framework for describing how disparity selectivity arises in primate and cat V1 is the disparity-energy model, which proposes that binocular complex cell responses result by summing and squaring binocular simple cell outputs (Ohzawa 1998; but see Burge J, Geisler WS, unpublished observations). In simple cells, binocular integration is modeled as a linear combination of left and right eye signals, followed by an output threshold nonlinearity. If the computation underlying disparity selectivity in mouse simple cells is the same as in the cat, the same model should provide accurate fits to mouse disparity tuning curves. Furthermore, this model could provide predictions of the synaptic inputs underlying monocular and binocular responses, which may reveal a relationship between ocular dominance and disparity selectivity that is not evident in spiking responses (Fig. 5).

To determine how effectively this model can account for the responses of mouse and cat V1 simple cells, we fit the following threshold-linear model to the monocular and binocular responses of individual neurons:

$$R(\phi) = \text{gain}\lfloor g_{\text{ipsi}}L_{\text{ipsi}}(\phi) + g_{\text{contra}}L_{\text{contra}}(\phi) - \text{thresh}\rfloor \quad (7)$$

where L_{ipsi} and L_{contra} are the luminance changes caused by the drifting grating for each eye (contralateral and ipsilateral) and g_{ipsi} and g_{contra} are the input gains from the ipsilateral and contralateral eyes. The gain represents the slope of the suprathreshold input to spiking transformation. The summed input from each eye is then passed through a threshold nonlinearity to generate a predicted spike rate. This model provides good fits to both the response amplitude and phase that occur in both mouse and cat V1 neurons for both monocular and binocular stimulation, even for neurons that are classified as monocular by ODI_R (Fig. 6*A*, mouse, $r^2 = 0.68$; Fig. 6*B*, cat, $r^2 = 0.71$). To account for the binocular response of these neurons, synaptic input from both eyes is required. The threshold-linear model (*Eq. 7*) fits these extracellular data by using a substantial degree of nonpreferred eye synaptic input, but not so much that a spiking response is observed to monocular stimulation (Fig. 6, *A* and *B*, monocular column). Binocular stimulation, however, reveals the impact of the synaptic input from the nonpreferred eye (Fig. 6, *A* and *B*, binocular column). Many mouse V1 neurons appear to be biased for the contralateral eye (Fig. 6*A*, monocular column), but weak input from the ipsilateral eye nonetheless strongly influenced responses during binocular stimulation (Fig. 6*A*, binocular column). The threshold-linear model is also able to capture simple cell disparity tuning from neurons that were classified as binocular by ocular dominance (data not shown).

In simple cells, the threshold-linear model accounted for binocular responses and disparity tuning in both mouse ($r^2 = 0.33 \pm 0.35$ SD) and cat ($r^2 = 0.60 \pm 0.52$ SD). To illustrate how well the model accounted for disparity selectivity, we plotted the predicted spiking responses (Fig. 6, *middle*) against the measured spiking responses (Fig. 6, *top*) for all simple cells, color-coded by the absolute value of ODI_R (Fig. 7, *A* and *B*). In simple cells, the threshold-linear model predicts the measured spiking responses, so much of the data lies along a unity line. The threshold-linear model is better able to capture the responses of cat than mouse simple cells, but this discrepancy is partly due to the overall differences in response modulation with disparity: for mouse neurons with DSI >0.15, the threshold-linear model captures far more of the response variance ($r^2 = 0.45 \pm 0.25$ SD).

We also fit the complex cell responses with the threshold-linear model. While the linear-threshold model could predict some binocular responses in mouse ($r^2 = 0.24 \pm 0.43$ SD), it was a poor predictor of response modulation in cat ($r^2 = 0.07 \pm 0.58$ SD). This model predicts response modulation to drifting gratings, while complex cells, by definition, do not modulate to drifting gratings.

At the level of spiking responses we did not observe a relationship between these two metrics of binocularity (ODI_R and DSI) (Fig. 8*A*; mouse: slope $= -0.07 \pm 0.08$, cat: slope $= -0.12 \pm 0.12$; principal component analysis with bootstrapped standard error), but such a relationship potentially exists at the subthreshold level and could be obscured in our extracellular measures. A strong prediction of the threshold-linear model is that a greater similarity in the gain of inputs from each eye, quantified by ODI based on synaptic inputs (ODI_V), should lead to a greater degree of disparity selectivity. To examine whether a relationship between the ocular dominance binocularity and disparity selectivity exists at the subthreshold level, we defined ODI_V as ocular dominance based on the synaptic input gains from the threshold-linear model:

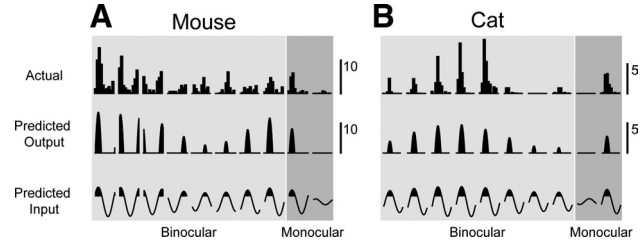

Fig. 6. A simple linear model predicts responses to dichoptic stimulation. Estimating input from each eye and using a threshold nonlinearity to model monocular responses in simple cells generates accurate predictions of binocular responses in mouse and cat. Example cells from Fig. 3*C* (*A*) and Fig. 3*D* (*B*) are shown. Measured responses (*top*) are shown with predicted responses (*middle*) and predicted subthreshold inputs (*bottom*) for both binocular and monocular responses. Scale bars indicate spike rate (spikes per second) for measured and predicted output.

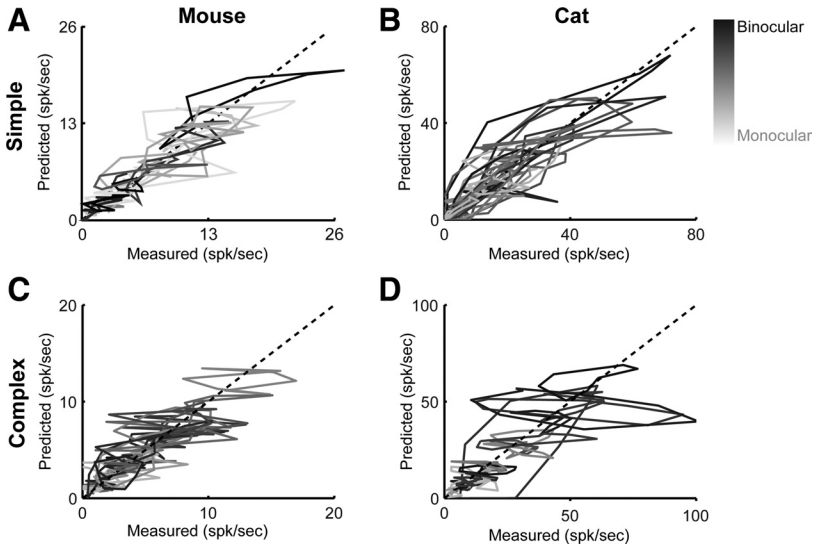

Fig. 7. Relationship between predicted and measured binocular responses. A simple linear-threshold model predicts binocular responses across simple cells recorded in mouse (*A* and *C*) and cat (*B* and *D*). Each cell is plotted and shaded relative to binocularity measured by monocular stimulation (absolute value of ODI). Dashed line represents unity.

$$\mathrm{ODI_V} = \frac{(g_{\mathrm{contra}} - g_{\mathrm{ipsi}})}{(g_{\mathrm{contra}} + g_{\mathrm{ipsi}})} \quad (8)$$

This comparison of $\mathrm{ODI_V}$ and DSI reveals a clear relationship across V1 simple cells (mouse: slope = −0.30 ± 0.12, cat: slope = −0.48 ± 0.14; principal component analysis with bootstrapped standard error). This finding indicates that, at a subthreshold level, the amount of input between the two eyes in response to a monocular stimulus is related to response modulation during binocular stimulation (Fig. 8*B*).

We considered whether the difference in the degree to which binocular disparity modulated the responses in mice and cats might be due to the differences in the binocularity of inputs: mice V1 neurons are more contralaterally biased than cat neurons than cat neurons. However, we find that mouse V1 neurons with matching degrees of input ocular dominance to cat neurons exhibit less disparity selectivity (Fig. 8*B*). Neurons with a substantial amount of binocular input ($\mathrm{ODI_V}$ = 0–0.25) were vastly different in disparity selectivity between the cat (mean = 0.49 ± 0.11 SD) and mouse (mean = 0.23 ± 0.06 SD) (Student's *t*-test, $P < 0.001$). Therefore the difference in the degree of disparity selectivity found in mouse and cat cannot solely reflect the contralateral bias of mouse neurons.

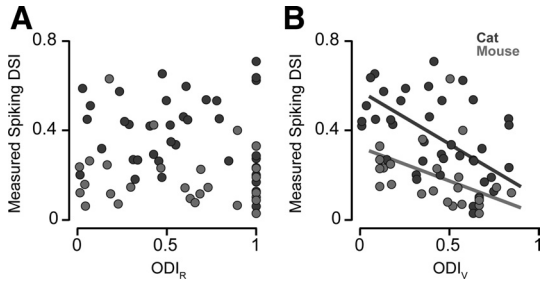

Fig. 8. Relationship of ODI from predicted inputs and measured DSI. *A*: the absolute value of the $\mathrm{ODI_R}$ of spiking responses is plotted with DSI for simple cells in cat (dark gray) and mouse (light gray). No clear relationship is evident. *B*: the absolute value of the $\mathrm{ODI_V}$, based on predicted subthreshold inputs, is plotted with DSI for simple cells in cat and mouse. Cells with predicted subthreshold inputs showing a greater degree of binocularity are also more selective for binocular disparities as measured by the spiking DSI. In both, the absolute value of ODI is plotted so that a value of 0 indicates a binocular neuron and a value of 1 indicates a monocular neuron.

DISCUSSION

Neurons in mouse V1 are known to receive inputs from left and right eye sensory streams, and yet it has been unclear how these two representations are integrated. By systematically changing the binocular disparity of left and right eye stimuli within an ecologically relevant range, we found that binocular integration in V1 neurons exhibited responses modulated by disparity. Indeed, disparity tuning in mouse V1 neurons is similar to that found in cat V1 neurons but differed in degree of modulation. A simple threshold-linear model accounted for the disparity selectivity of simple cells in both the cat and the mouse, suggesting that a substantial subthreshold input from the weaker eye significantly modulates responses during normal binocular viewing. Our recordings demonstrate that a common computation is being performed by V1 across mammalian species that provides information about the depth of objects.

Our initial experiments revealed an increase in neuronal sensitivity to binocular stimuli, but the increase is less than expected under the assumption of independent sources of noise in the sensory periphery (Simpson et al. 2009). Human psychophysical detection performance generally improves by a factor of $\sqrt{2}$ with binocular versus monocular stimulation. These experiments are generally performed at threshold contrast; sensitivity is generally smaller when the task is to discriminate differences between high-contrast gratings (Legge 1984). Because our measurements in the mouse were performed at high contrast, however, our records may not reveal the expected sensitivity improvement of $\sqrt{2}$. Measuring increases in sensitivity in mouse V1 neurons with low-contrast stimuli may better match psychophysical measurements.

A wide variety of binocular interactions are present in mouse V1 neurons, as previously shown in cat V1 neurons (Ohzawa and Freeman 1986; Pettigrew et al. 1968). One of these interactions is the dramatic response amplitude difference between monocular and binocular responses (Fig. 3, *B* and *C*, and Fig. 6, *A* and *B*). Many mouse V1 neurons are clearly modulated by binocular stimulation, even though they would be classified as monocular by conventional measures of ocular dominance. A simple explanation is that subthreshold synaptic inputs exist for both eyes but monocular input from one eye is

not sufficiently weighted to exceed the spiking threshold under monocular stimulation (Priebe and Ferster 2008). Near spike threshold, small changes in membrane potential or synaptic input generate huge changes in spike rate, so amplitude differences between monocular and binocular synaptic inputs could elicit vastly different spiking responses. This explanation suggests that disparity tuning results from interactions at the level of subthreshold membrane potential, hidden from our extracellular records (Ohzawa 1998; Ohzawa and Freeman 1986).

Mammals are not the only vertebrates possessing binocular neurons, but the structure of the mammalian visual system contains elements supporting the generation of binocular neurons. Unlike other vertebrates, not all retinal ganglion cell projections cross at the optic chiasm. Both left and right eye outputs project to the same brain structures, instead of being laterally segregated. In the primate, for example, ~40% of the ipsilateral retinal projections do not cross at the optic chiasm, allowing for information streams from both eyes to innervate the same side of the lateral geniculate nucleus (LGN) (Chalupa and Lia 1991; Perry et al. 1984). The percentage of retinal ganglion cell projections not crossing the optic chiasm in the mouse is very small, ~3–4%, but that small percentage of uncrossed retinal output innervates 10% of mouse LGN (Dräger 1974; Godement et al. 1984). Although ipsilateral and contralateral retinal ganglion cells project to the LGN, those projections remain segregated. The second structural change in the visual system of mammals is the presence of a six-layer cerebral cortex where left and right eye signals converge. Like the expansion of the ipsilateral representation in the LGN from a few ipsilateral retinal ganglion cells, the mouse binocular zone occupies approximately one-third of V1 despite an ipsilateral representation of only 10% in the LGN (Leamey and Protti 2008). In the mouse it appears that a small basis for binocularity, in terms of uncrossed ipsilateral retinal projections, is amplified greatly to generate binocularity in V1. The weakness of the ipsilateral projection is evident in the monocular bias toward the contralateral eye (Fig. 5). It does not appear, however, that this contralateral bias of input to V1 accounts for the weaker disparity selectivity observed in mouse V1 relative to cat V1: comparing mouse and cat neurons with similar input ocular dominance (as reflected in ODI_v) reveals that mouse neurons are systematically less sensitive to disparity than cat neurons (Fig. 8*B*). So the difference in ocular dominance between cat and mouse does not account for the difference in the degree of disparity tuning.

Throughout our study we find less prominent disparity tuning in mouse V1 neurons compared with those in cat (Fig. 5), even when examining only simple cells (Fig. 8*B*). In general, mouse V1 neurons are modulated to a lesser degree than cat neurons, although the potential exists for large disparity selectivity as we find that DSI values share a similar range (mouse: 0–0.7, cat: 0–0.75). One reason for these differences could be the lack of ocular dominance columns in mouse V1, where instead there is a single binocular region receiving inputs from the ipsilateral eye. At the edges of this region neurons could be weakly binocular even at the level of synaptic input. Another difference is the extent of receptive fields relative to the binocular zone. Since receptive field sizes in mouse V1 vary greatly (5–30°) and the binocular field of view in mice is only 40° (Fig. 2*B*), it is possible that binocular overlap in many neurons is too small in order to generate the striking binocular response interactions observed in cat. In addition, simple cell receptive fields in mouse V1 neurons are shown to differ from those in cat, as there is substantial overlap between ON and OFF subregions (Liu et al. 2010). In cat V1, simple cells of layer 4 receive direct input from the LGN and are thought to form the basis of disparity selectivity, which is inherited by complex cells in layers 2/3 through the integration of inputs across simple cells (Ohzawa 1998). Simple and complex cells of mouse V1 are found throughout cortical layers (Niell and Stryker 2008), suggesting that the emergence of disparity sensitivity could occur through a number of mechanisms and may not require direct thalamocortical input. The synaptic basis for binocular integration in mouse V1 may be a combination of thalamocortical, intracortical, and inhibitory synaptic input. In cat V1 simple cells, the linear summation of binocular inputs (Scholl and Priebe 2011) leads to robust disparity tuning (Ohzawa and Freeman 1986). In mouse simple cells, however, the summation of binocular inputs may be nonlinear. Another possibility is that while linear summation of binocular inputs appears to prevail in cat V1 simple cells (Scholl and Priebe 2011) and generates robust disparity tuning (Ohzawa and Freeman 1986), summation of binocular inputs in mouse simple cells is nonlinear. Consistent with this hypothesis, it is known that mouse V1 neurons possess a push-push excitation-inhibition mechanism (Liu et al. 2010; Tan et al. 2011) while cat V1 neurons exhibit a push-pull mechanism (Hirsch et al. 1998; Priebe and Ferster 2006). It may be that this difference in receptive field organization underlies the different binocular integration observed in the mouse and the cat.

Other vertebrates besides mammals have evolved visual systems with binocular neurons. One prominent example, the barn owl (*Tyto alba*), has binocular depth perception that is quite similar to human binocular depth perception (van der Willigen 2011). Binocular neurons in the barn owl's wulst visual area have a high degree of binocularity and disparity tuning (Pettigrew and Konishi 1976a; Nieder and Wagner 2000, 2001) and exhibit a number of properties similar to those shown in mouse (and primate and cat) V1 binocular neurons: strong disparity tuning, enhancement and suppression of responses to binocular stimulation, and ocular dominance plasticity during the critical period (Pettigrew and Konishi 1976b). Given these similarities, it is interesting to note that binocularity in birds evolved independently from that in mammals (Pettigrew 1986). Indeed, disparity selectivity in the barn owl emerges from a visual pathway that is completely different from that in mammals. In contrast to mammals, in the barn owl projections from the two eyes cross at the optic chiasm and remain segregated until they converge within the wulst.

Many animals with binocular depth perception use multiple visual depth cues to estimate depth (Hillis et al. 2004; Landy et al. 1995). These signals include but are not limited to figure-ground cues (Burge et al. 2010), defocus blur (Burge and Geisler 2011; Held et al. 2012), motion parallax (Wallace 1959), and looming (Beverley 1973; Beverley and Regan 1973). Binocular disparity is thus not the only source of information relevant for estimating depth, but it is a source of information that many animals exploit.

The convergent evolution of binocular depth perception suggests that stereopsis confers important evolutionary advantages. Binocular neurons that underlie this perceptual ability across phyla have similar properties despite significant differ-

ences in the neuroanatomical pathways and the (presumed) different mechanisms that give rise to them. This suggests that binocular neurons subserving depth perception extract similar information from the retinal images and that a common computation, independent of a particular mechanism, may underlie all visual systems with stereopsis (Burge J, Geisler WS, unpublished observations). It is not yet known whether, or how, rodents use disparity to estimate depth in natural viewing: the necessary psychophysical studies have not been performed. It may be, for example, that the upper and overhead retinotopic regions of mouse vision play an important role in predator avoidance behaviors. Nonetheless, our recordings demonstrate that mouse V1 neurons are sensitive to binocular disparities consistent with an ecologically relevant range of object depths. The cross-species similarities between mouse, owl, cat, and primate suggest that the integration of left- and right-eye image information underlying disparity selectivity is an example of a common computation performed across visual systems. This computation is an important example of how visual systems select for and integrate useful information from multiple sensory sources to constrain estimates of behaviorally relevant properties of the natural environment.

ACKNOWLEDGMENTS

We are grateful to Jessica Hanover and Alex Huk for helpful discussions and comments.

GRANTS

This work was supported by grants from the National Eye Institute (EY-019288) and The Pew Charitable Trusts.

DISCLOSURES

No conflicts of interest, financial or otherwise, are declared by the author(s).

AUTHOR CONTRIBUTIONS

Author contributions: B.S., J.B., and N.J.P. conception and design of research; B.S., J.B., and N.J.P. performed experiments; B.S. and J.B. analyzed data; B.S., J.B., and N.J.P. interpreted results of experiments; B.S. and J.B. prepared figures; B.S., J.B., and N.J.P. drafted manuscript; B.S., J.B., and N.J.P. edited and revised manuscript; B.S., J.B., and N.J.P. approved final version of manuscript.

REFERENCES

Anderson PA, Movshon JA. Binocular combination of contrast signals. *Vision Res* 29: 1115–1132, 1989.

Banks MS, Bennett PJ. Optical and photoreceptor immaturities limit the spatial and chromatic vision of human neonates. *J Opt Soc Am A* 5: 2059–2079, 1988.

Barlow HB, Blakemore C, Pettigrew JD. The neural mechanism of binocular depth discrimination. *J Physiol* 193: 327–342, 1967.

Beverley KI. Disparity detectors in human depth perception: evidence for directional selectivity. *Science* 181: 877–879, 1973.

Beverley KI, Regan D. Selective adaptation in stereoscopic depth perception. *J Physiol* 232: 40P–41P, 1973.

Blakemore C. Binocular depth discrimination and the nasotemporal division. *J Physiol* 205: 471–497, 1969.

Blakemore C. The range and scope of binocular depth discrimination in man. *J Physiol* 211: 599–622, 1970.

Bonin V, Histed MH, Yurgenson S, Reid RC. Local diversity and fine-scale organization of receptive fields in mouse visual cortex. *J Neurosci* 31: 18506–18521, 2011.

Brainard DH. The Psychophysics Toolbox. *Spat Vis* 10: 443–446, 1997.

Burge J, Geisler WS. Optimal defocus estimation in individual natural images. *Proc Natl Acad Sci USA* 108: 16849–16854, 2011.

Burge J, Fowlkes CC, Banks MS. Natural-scene statistics predict how the figure-ground cue of convexity affects human depth perception. *J Neurosci* 30: 7269–7280, 2010.

Chalupa LM, Lia B. The nasotemporal division of retinal ganglion cells with crossed and uncrossed projections in the fetal rhesus monkey. *J Neurosci* 11: 191–202, 1991.

Chalupa LM, Williams RW. *Eye, Retina, and Visual System of the Mouse*. Cambridge, MA: MIT Press, 2008.

Chino YM, Smith EL, Yoshida K, Cheng H, Hamamoto J. Binocular interactions in striate cortical neurons of cats reared with discordant visual inputs. *J Neurosci* 14: 5050–5067, 1994.

Dräger UC. Autoradiography of tritiated proline and fucose transported transneuronally from the eye to the visual cortex in pigmented and albino mice. *Brain Res* 82: 284–292, 1974.

Dräger UC. Receptive fields of single cells and topography in mouse visual cortex. *J Comp Neurol* 160: 269–290, 1975.

Field DJ. Relations between the statistics of natural images and the response properties of cortical cells. *J Opt Soc Am A* 4: 2739–2394, 1987.

Gao E, DeAngelis GC, Burkhalter A. Parallel input channels to mouse primary visual cortex. *J Neurosci* 30: 5912–5926, 2010.

Godement P, Salaün J, Imbert M. Prenatal and postnatal development of retinogeniculate and retinocollicular projections in the mouse. *J Comp Neurol* 230: 552–575, 1984.

Gordon JA, Stryker MP. Experience-dependent plasticity of binocular responses in the primary visual cortex of the mouse. *J Neurosci* 16: 3274–3286, 1996.

Hanover JL, Huang ZJ, Tonegawa S, Stryker MP. Brain-derived neurotrophic factor overexpression induces precocious critical period in mouse visual cortex. *J Neurosci* 19: RC40, 1999.

Held RT, Cooper EA, Banks MS. Blur and disparity are complementary cues to depth. *Curr Biol* 22: 426–431, 2012.

Heesy CP. On the relationship between orbit orientation and binocular visual field overlap in mammals. *Anat Rec A* 281A: 1104–1110, 2004.

Hillis JM, Watt SJ, Landy MS. Slant from texture and disparity cues: optimal cue combination. *J Vis* 4:967–992, 2004.

Hirsch JA, Alonso JM, Reid RC, Martinez LM. Synaptic integration in striate cortical simple cells. *J Neurosci* 18: 9517–9528, 1998.

Hofer SB, Mrsic-Flogel TD, Bonhoeffer T, Hübener M. Prior experience enhances plasticity in adult visual cortex. *Nat Neurosci* 9: 127–132, 2006.

Hubel DH, Wiesel TN. Receptive fields, binocular interaction and functional architecture in the cat's visual cortex. *J Physiol* 160: 106–154, 1962.

Hubel DH, Wiesel TN. A re-examination of stereoscopic mechanisms in area 17 of the cat. *J Physiol* 232: 29P–30P, 1973.

Huberman AD, Niell CM. What can mice tell us about how vision works? *Trends Neurosci* 34: 464–473, 2011.

Joshua DE. Binocular single vision and depth discrimination. Receptive field disparities for central and peripheral vision and binocular interaction on peripheral single units in cat. *Exp Brain Res* 10: 389–416, 1970.

Kalatsky VA, Stryker MP. New paradigm for optical imaging: temporally encoded maps of intrinsic signal. *Neuron* 38: 529–545, 2003.

de la Cera EG, Rodríguez G, Llorente L, Schaeffel F, Marcos S. Optical aberrations in the mouse eye. *Vision Res* 46: 2546–2553, 2006.

Landy MS, Maloney LT, Johnston EB. Measurement and modeling of depth cue combination: in defense of weak fusion. *Vision Res* 35: 389–412, 1995.

Leamey CA, Protti DA. Comparative survey of the mammalian visual system with reference to the mouse. In: *Eye, Retina, and Visual System of the Mouse*. Cambridge, MA: MIT Press, 2008.

Legge GE. Binocular contrast summation. I. Detection and discrimination. *Vision Res* 24: 373–383, 1984.

LeVay S, Voigt T. Ocular dominance and disparity coding in cat visual cortex. *Vis Neurosci* 1: 395–414, 1988.

Liu B, Li P, Sun YJ, Li Y, Zhang LI, Tao HW. Intervening inhibition underlies simple-cell receptive field structure in visual cortex. *Nat Neurosci* 13: 89–96, 2010.

Mangini NJ, Pearlman AL. Laminar distribution of receptive field properties in the primary visual cortex of the mouse. *J Comp Neurol* 193: 203–222, 1980.

Métin C, Godement P, Imbert M. The primary visual cortex in the mouse: receptive field properties and functional organization. *Exp Brain Res* 69: 594–612, 1988.

Mrsic-Flogel TD, Hofer SB, Ohki K, Reid RC, Bonhoeffer T, Hübener M. Homeostatic regulation of eye-specific responses in visual cortex during ocular dominance plasticity. *Neuron* 54: 961–972, 2007.

Nieder A, Wagner H. Horizontal-disparity tuning of neurons in the visual forebrain of the behaving barn owl. *J Neurophysiol* 83: 2967–2979, 2000.

Nieder A, Wagner H. Hierarchical procession of horizontal disparity information in the visual forebrain of behaving owls. *J Neurosci* 21: 4514–4522, 2001.

Niell CM, Stryker MP. Highly selective receptive fields in mouse visual cortex. *J Neurosci* 28: 7520–7536, 2008.

Nikara T, Bishop PO, Pettigrew JD. Analysis of retinal correspondence by studying receptive fields of binocular single units in cat striate cortex. *Exp Brain Res* 6: 353–372, 1968.

Ohzawa I. Mechanisms of stereoscopic vision: the disparity energy model. *Curr Opin Neurobiol* 8: 509–515, 1998.

Ohzawa I, Freeman RD. The binocular organization of simple cells in the cat's visual cortex. *J Neurophysiol* 56: 221–242, 1986.

Packwood J, Gordon B. Stereopsis in normal domestic cat, Siamese cat, and cat raised with alternating monocular occlusion. *J Neurophysiol* 38: 1485–1499, 1975.

Pardhan S, Rose D. Binocular and monocular detection of Gabor patches in binocular two-dimensional noise. *Perception* 28: 203–215, 1999.

Pelli DG. The VideoToolbox software for visual psychophysics: transforming numbers into movies. *Spat Vis* 10: 437–442, 1997.

Perry VH, Oehler R, Cowey A. Retinal ganglion cells that project to the dorsal lateral geniculate nucleus in the macaque monkey. *Neuroscience* 12: 1101–1123, 1984.

Pettigrew JD. Evolution of binocular vision. In: *Visual Neuroscience*, edited by Pettigrew JD, Sanderson KJ, Levick WR. Cambridge, UK: Cambridge Univ. Press, 1986, p. 208–222.

Pettigrew J, Konishi M. Neurons selective for orientation and binocular disparity in the visual Wulst of the barn owl (*Tyto alba*). *Science* 193: 675–678, 1976a.

Pettigrew JD, Konishi M. Effect of monocular deprivation on binocular neurones in the owl's visual Wulst. *Nature* 264: 753–754, 1976b.

Pettigrew JD, Nikara T, Bishop PO. Binocular interaction on single units in cat striate cortex: simultaneous stimulation by single moving slit with receptive fields in correspondence. *Exp Brain Res* 6: 391–410, 1968.

Priebe NJ. The relationship between subthreshold and suprathreshold ocular dominance in cat primary visual cortex. *J Neurosci* 28: 8553–8559, 2008.

Priebe NJ, Ferster D. Mechanisms underlying cross-orientation suppression in cat visual cortex. *Nat Neurosci* 9: 552–561, 2006.

Priebe NJ, Ferster D. Inhibition, spike threshold, and stimulus selectivity in primary visual cortex. *Neuron* 57: 482–497, 2008.

Ringach DL, Shapley RM, Hawken MJ. Orientation selectivity in macaque V1: diversity and laminar dependence. *J Neurosci* 22: 5639–5651, 2002.

Sarnaik R, Wang BS, Cang J. Experience-dependent and independent binocular correspondence of receptive field subregions in mouse visual cortex. *Cereb Cortex* (February 6, 2013). doi: 10.1093/cercor/bht027.

Scholl B, Priebe NJ. Monocular inputs linearly combine to generate binocular responses in simple cells of primary visual cortex (Abstract). Society for Neuroscience Annual Meeting, 2011.

Schuett S, Bonhoeffer T, Hübener M. Mapping retinotopic structure in mouse visual cortex with optical imaging. *J Neurosci* 22: 6549–6559, 2002.

Simpson AJ, Fitter MJ. What is the best index of detectability? *Psychol Bull* 80: 481–488, 1973.

Simpson WA, Manahilov V, Shahani U. Two eyes: square root 2 better than one? *Acta Psychol (Amst)* 131: 93–98, 2009.

Swets JA. Form of empirical ROCs in discrimination and diagnostic tasks: implications for theory and measurement of performance. *Psychol Bull* 99: 181–198, 1986.

Tagawa Y, Kanold PO, Majdan M, Shatz CJ. Multiple periods of functional ocular dominance plasticity in mouse visual cortex. *Nat Neurosci* 8: 380–388, 2005.

Tan AY, Brown BD, Scholl B, Mohanty D, Priebe NJ. Orientation selectivity of synaptic input to neurons in mouse and cat primary visual cortex. *J Neurosci* 31: 12339–12350, 2011.

Vreysen S, Zhang B, Chino YM, Arckens L, Van den Bergh G. Dynamics of spatial frequency tuning in mouse visual cortex. *J Neurophysiol* 107: 2937–2949, 2012.

Wagor E, Mangini NJ, Pearlman AL. Retinotopic organization of striate and extrastriate visual cortex in the mouse. *J Comp Neurol* 193: 187–202, 1980.

Wallace GK. Visual scanning in the desert locust *Schistocerca gregaria* Forskål. *J Exp Biol* 36: 512–525, 1959.

Wang BS, Sarnaik R, Cang J. Critical period plasticity matches binocular orientation preference in the visual cortex. *Neuron* 65: 246–256, 2010.

van der Willigen RF, Frost BJ, Wagner H. Stereoscopic depth perception in the owl. *Neuroreport* 9: 1233–1237, 1998.